Production of pseudoscalar and scalar quarkonia in a light front approach

Wolfgang Schäfer [1]

[1] Institute of Nuclear Physics, PAN, Kraków

Środowiskowe Seminarium Fizyki Wysokich Energii "Białasówka", 27. 3. 2020

Outline

Introduction

$\gamma^*\gamma^* \to \eta_c(1S, 2S), \chi_{c0}$ transition form factors: light front description

k_T-factorization formulation: off-shell matrix element

η_c: Results for LHCb kinematics - "forward production"

η_c: Results for ATLAS/CMS kinematics - "central production"

χ_{c0}: Results for transition form factors and hadroproduction

Conclusions


I. Babiarz, R. Pasechnik, W. S. and A. Szczurek, "Hadroproduction of scalar P-wave quarkonia in the light-front k_T-factorization approach," arXiv:2002.09352 [hep-ph].


I. Babiarz, R. Pasechnik, W. S. and A. Szczurek, "Prompt hadroproduction of $\eta_c(1S, 2S)$ in the k_T-factorization approach," JHEP **2002**, 037 (2020) [arXiv:1911.03403 [hep-ph]].


I. Babiarz, V. P. Goncalves, R. Pasechnik, W. S. and A. Szczurek, "$\gamma^*\gamma^* \to \eta_c(1S, 2S)$ transition form factors for spacelike photons," Phys. Rev. D **100**, no. 5, 054018 (2019) [arXiv:1908.07802 [hep-ph]].

Introduction

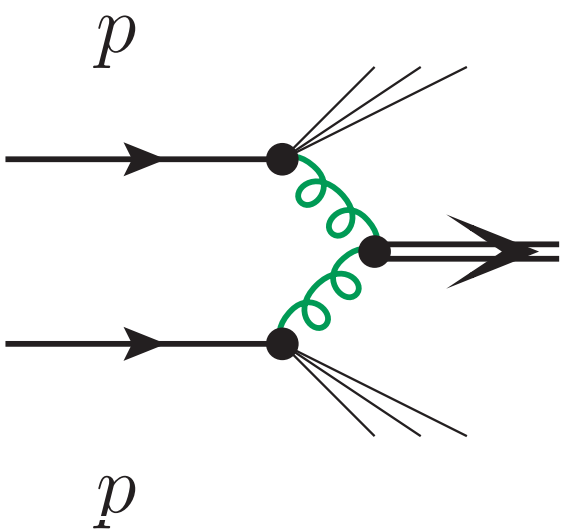

$\eta_{c,b}$, $\chi_{c,b}$

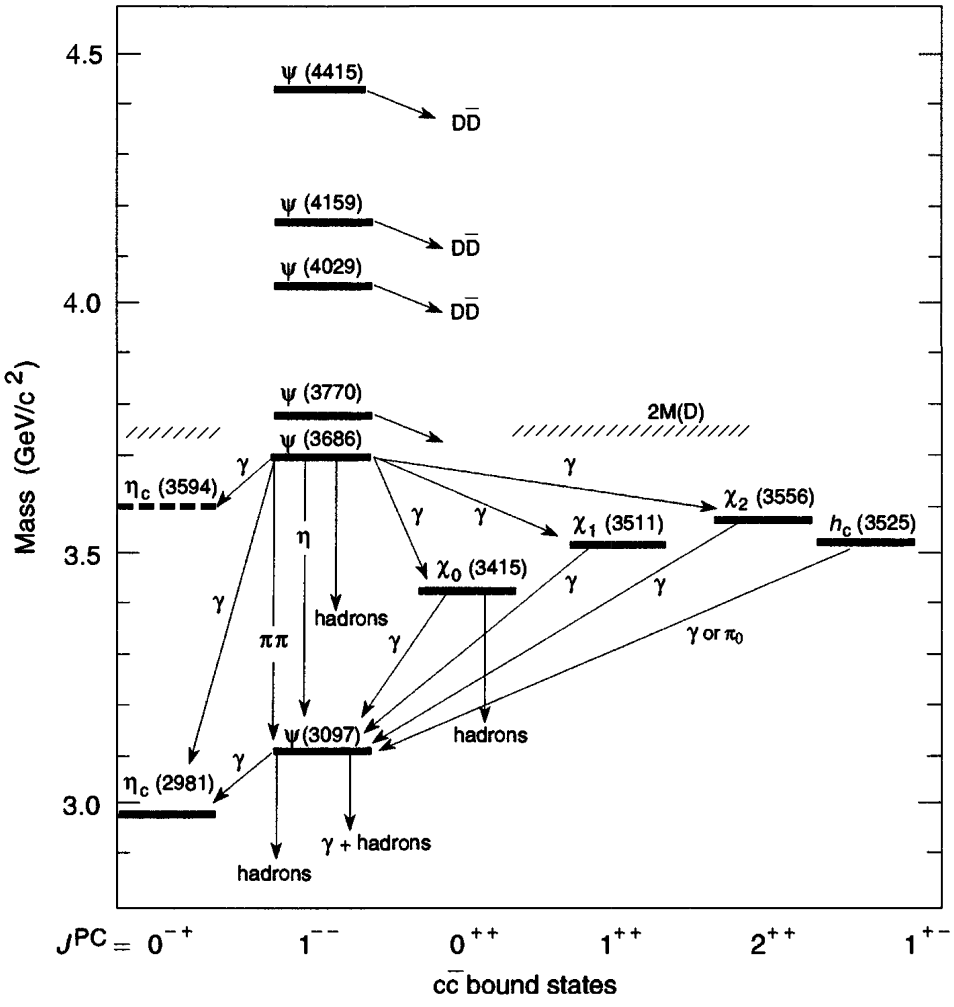

- Even C-parity quarkonia ($c\bar{c}$ or $b\bar{b}$ states) : prompt production via gluon-gluon fusion.
- a good probe for transverse momentum dependent gluon densities. In k_T factorization: need off shell matrix element for the fusion of two spacelike virtual gluons.

Description of the mechanism $\gamma^*\gamma^* \to \eta_c(1S, 2S)$

Production of η_c in double-tagged e^+e^- collisions measures the $\gamma^*\gamma^*\eta_c$ transition form factor.

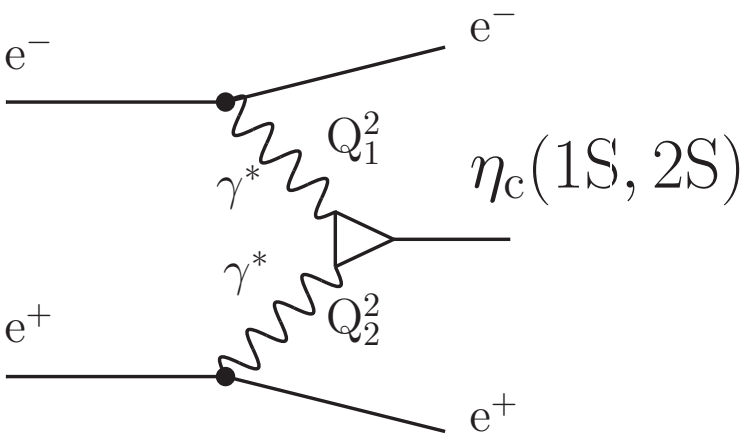

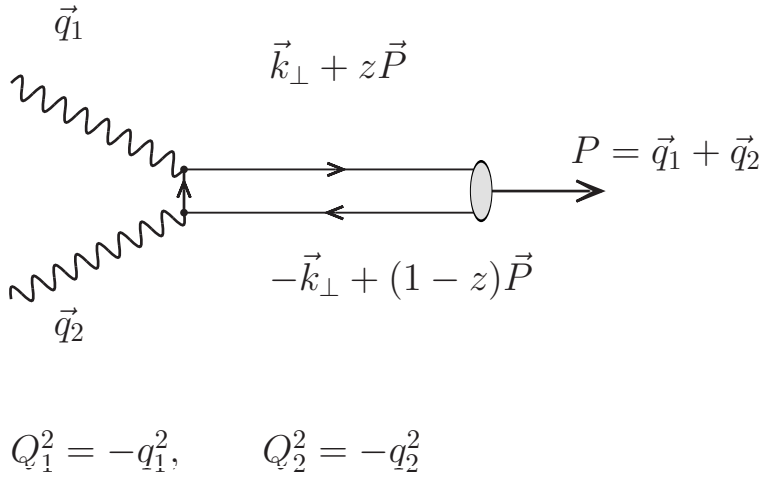

$$\mathcal{M}_{\mu\nu}(\gamma^*(q_1)\gamma^*(q_2) \to \eta_c) = 4\pi\alpha_{\rm em}\,(-i)\varepsilon_{\mu\nu\alpha\beta}\,q_1^\alpha q_2^\beta\, F(Q_1^2, Q_2^2)$$

Light-front representation of the transition form factor:

$$F(Q_1^2, Q_2^2) = e_c^2\sqrt{N_c}4m_c \cdot \int \frac{dzd^2\mathbf{k}}{z(1-z)16\pi^3}\psi(z,\mathbf{k})$$

$$\left\{\frac{1-z}{(\mathbf{k}-(1-z)\mathbf{q}_2)^2 + z(1-z)\mathbf{q}_1^2 + m_c^2} + \frac{z}{(\mathbf{k}+z\mathbf{q}_2)^2 + z(1-z)\mathbf{q}_1^2 + m_c^2}\right\}.$$

$\gamma^*\gamma^* \to M,\ M = \eta_c(1S, 2S), \chi_{c0}$

$$\mathcal{M}_{\mu\nu} = \int \frac{dzd^2\boldsymbol{k}}{z(1-z)16\pi^3} \sum_{\lambda,\bar{\lambda}} \Psi^*_{\lambda\bar{\lambda}}(z,\boldsymbol{k}) \mathcal{M}^{\lambda\bar{\lambda}}_{\mu\nu}(\gamma^*\gamma^* \to Q_\lambda(zP_+, \boldsymbol{p}_Q)\bar{Q}_{\bar{\lambda}}((1-z)P_+, \boldsymbol{p}_{\bar{Q}}) \,.$$

General form of the amplitude – invariant form factors:

- pseudoscalar:

$$\frac{1}{4\pi\alpha_{\rm em}} \mathcal{M}_{\mu\nu}(\gamma^*(q_1)\gamma^*(q_2) \to \eta_c) = (-i)\varepsilon_{\mu\nu\alpha\beta} q_1^\alpha q_2^\beta \, F(Q_1^2, Q_2^2)$$

- scalar:

$$\frac{1}{4\pi\alpha_{\rm em}} \mathcal{M}_{\mu\nu}(\gamma^*(q_1)\gamma^*(q_2) \to \chi_{c0}) = -\underbrace{\delta^\perp_{\mu\nu}(q_1,q_2)\, F_{TT}(Q_1^2, Q_2^2)}_{\text{transverse}} + \underbrace{e^L_\mu(q_1) e^L_\nu(q_2)\, F_{LL}(Q_1^2, Q_2^2)}_{\text{longitudinal}} \,.$$

- we can extract the invariant form factors by calculating the projection on light-front directions

$$n^{+\mu} n^{-\nu} \mathcal{M}_{\mu\nu} \text{ in the frame } q_{1\mu} = q_1^+ n^+_\mu + q^\perp_{1\mu}, q_{2\mu} = q_2^- n^-_\mu + q^\perp_{2\mu},$$

Light-front wave functions

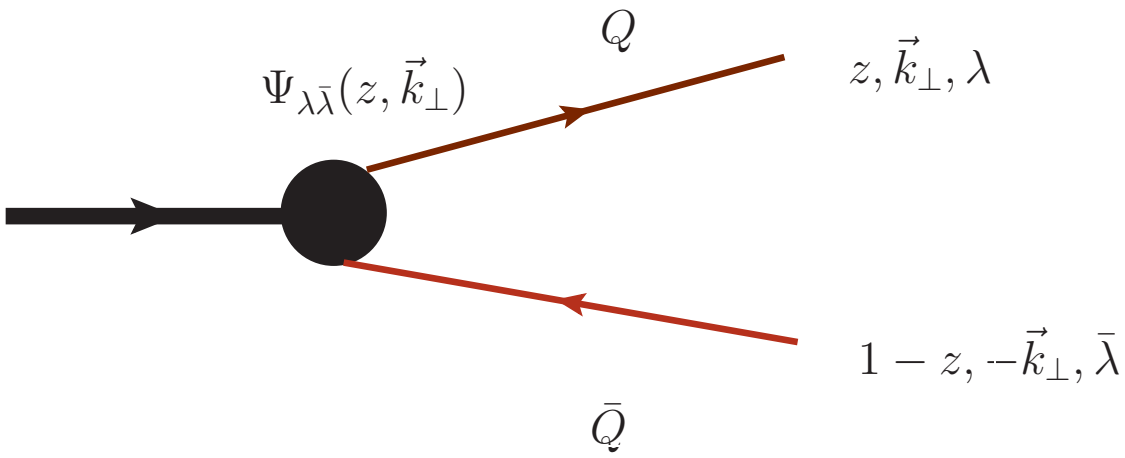

Frame-independent $Q\bar{Q}$ component from LF-Fock-state expansion:

$$|\text{Meson};P_+,\mathbf{P}\rangle = \sum_{i,j,\lambda,\bar{\lambda}} \frac{\delta^i_j}{\sqrt{N_c}} \int \frac{dzd^2\mathbf{k}}{z(1-z)16\pi^3} \Psi_{\lambda\bar{\lambda}}(z,\mathbf{k})|Q_{i\lambda}(zP_+,\mathbf{p}_Q)\bar{Q}^j_{\bar{\lambda}}((1-z)P_+,\mathbf{p}_{\bar{Q}})\rangle + \ldots$$

- z=fraction of meson's plus-momentum carried by quark, $\boldsymbol{k} = (1-z)\boldsymbol{p}_Q - z\boldsymbol{p}_{\bar{Q}}$
- dominance of 2-body Fock state:

$$\sum_{\lambda,\bar{\lambda}} \int \frac{dzd^2\mathbf{k}}{z(1-z)16\pi^3} |\Psi_{\lambda\bar{\lambda}}(z,\mathbf{k})|^2 = N_{Q\bar{Q}} \sim 1.$$

- We ideally would like to use LFWF's from a direct formulation of the bound-state eqn's on the LF. For the time being we use a prescription based on the rest-frame WF.

LF wave functions from RF – Terentev prescription

Rest-frame wave functions for $J = 0$:

$$\Psi_{\tau\bar{\tau}}(\vec{k}) \quad = \quad \underbrace{\frac{1}{\sqrt{2}}\xi_Q^{\tau\dagger}\,\hat{\mathcal{O}} i\sigma_2\,\xi_{\bar{Q}}^{\bar{\tau}*}}_{\text{spin}-\text{orbit}}\;\underbrace{\frac{u_L(k)}{k}}_{\text{radial}}\;\frac{1}{\sqrt{4\pi}};\ \text{where}\hat{\mathcal{O}} = \begin{cases} \mathbb{I} & \text{spin-singlet, } S=0, L=0. \\ \frac{\vec{\sigma}\cdot\vec{k}}{k}, & \text{spin-triplet, } S=1, L=1. \end{cases}$$

- mapping RF momentum to LF representation:

$$\vec{k} = (\boldsymbol{k}, k_z) = (\boldsymbol{k}, \frac{1}{2}(2z-1)M)\,, \text{with } M^2 = \frac{\boldsymbol{k}^2 + m_Q^2}{z(1-z)}.$$

- Melosh-trf of spin-orbit part:

$$\xi_Q = R(z,\boldsymbol{k})\chi_Q,\ \xi^*_{\bar{Q}} = R^*(1-z,-\boldsymbol{k})\chi^*_{\bar{Q}} \text{ with } R(z,\boldsymbol{k}) = \frac{m_Q + zM - i\vec{\sigma}\cdot(\vec{n}\times\boldsymbol{k})}{\sqrt{(m_Q+zM)^2+\boldsymbol{k}^2}}$$

$$\hat{\mathcal{O}}' = R^\dagger(z,\boldsymbol{k})\mathcal{O}\,i\sigma_2 R^*(1-z,-\boldsymbol{k})(i\sigma_2)^{-1} = R^\dagger(z,\boldsymbol{k})\hat{\mathcal{O}}\,R(1-z,-\boldsymbol{k})\,.$$

- including a jacobian for the transition to LF momenta, we can finally transform

$$\Psi_{\tau\bar{\tau}}(\vec{k}) \to \Psi_{\lambda\bar{\lambda}}(z,\boldsymbol{k})\,.$$

Light front wave functions after Melosh-transform

Scalar (P-wave)

$$\begin{aligned}\Psi_{\lambda\bar{\lambda}}(z,\boldsymbol{k}) &= \begin{pmatrix}\Psi_{++}(z,\boldsymbol{k}) & \Psi_{+-}(z,\boldsymbol{k})\\ \Psi_{-+}(z,\boldsymbol{k}) & \Psi_{--}(z,\boldsymbol{k})\end{pmatrix}\\ &= \frac{-1}{\sqrt{z(1-z)}}\begin{pmatrix}k_x-ik_y & m_Q(1-2z)\\ m_Q(1-2z) & -k_x-ik_y\end{pmatrix}\psi_P(z,\boldsymbol{k})\,.\end{aligned}$$

Pseudoscalar (S-wave)

$$\Psi_{\lambda\bar{\lambda}}(z,\boldsymbol{k}) = \frac{1}{\sqrt{z(1-z)}}\begin{pmatrix}-k_x+ik_y & m_Q\\ -m_Q & -k_x-ik_y\end{pmatrix}\psi_S(z,\boldsymbol{k})\,.$$

- Note that in the NR limit, the pseudoscalar has only the component with antiparallel helicities, whereas after Melosh transform also parallel helicities appear.

Nonrelativistic quarkonium wave functions

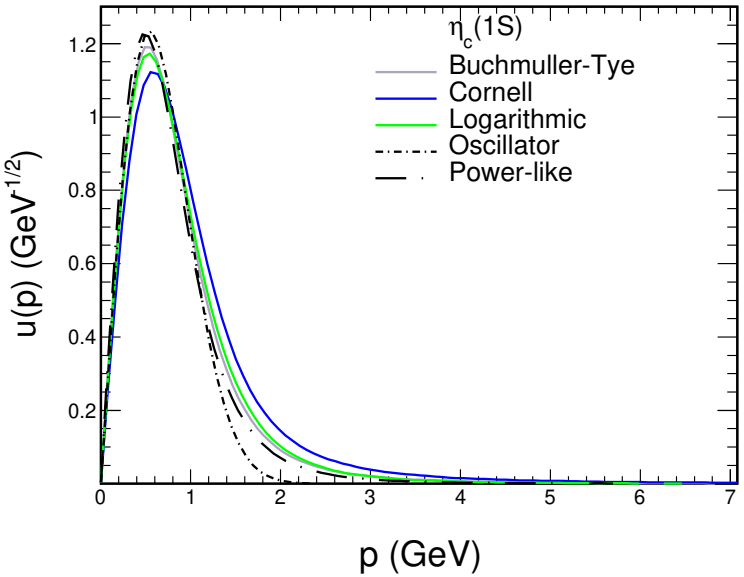

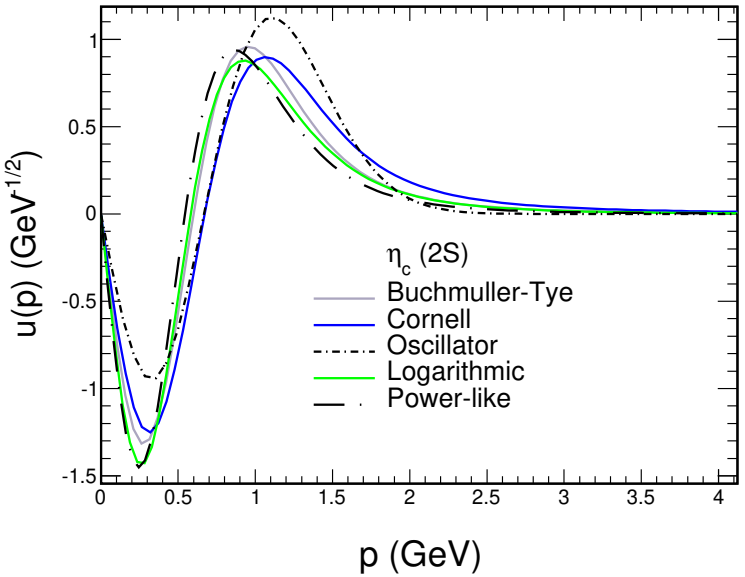

Radial momentum space wave function for different potentials.

Radial wave function are obtained from the Schrödinger equation

J. Cepila, J. Nemchik, M. Krelina and R. Pasechnik, Eur. Phys. J. C **79**, no. 6, 495 (2019).

$$\frac{\partial^2 u(r)}{\partial r^2} = (V_{\rm eff}(r) - \epsilon)u(r)\,, \qquad u(r) = \sqrt{4\pi}\, r\psi(r)\,, \quad u(p) = \sqrt{\frac{2}{\pi}} \int_0^\infty r dr j_0(pr) u(r)$$

$$\Psi_{\sigma\bar{\sigma}}(\vec{p}) = \underbrace{\frac{1}{\sqrt{2}} \chi^\dagger_\sigma i\sigma_2 \chi_{\bar{\sigma}}}_{\rm spin-singlet} \underbrace{\frac{u(p)}{p} \frac{1}{\sqrt{4\pi}}}_{\rm s-wave}\,.$$

Light-front wave functions

Frame-independent $q\bar{q}$ component from LF-Fock-state expansion:

$$|\eta_c; P_+, \mathbf{P}\rangle = \sum_{i,j,\lambda,\bar{\lambda}} \frac{\delta^i_j}{\sqrt{N_c}} \int \frac{dz d^2\mathbf{k}}{z(1-z)16\pi^3} \Psi_{\lambda\bar{\lambda}}(z,\mathbf{k}) |c_{i\lambda}(zP_+, \mathbf{p}_c) \bar{c}^j_{\bar{\lambda}}((1-z)P_+, \mathbf{p}_{\bar{c}})\rangle + \ldots$$

$$\Psi_{\lambda\bar{\lambda}}(z,\mathbf{k}) = \bar{u}_\lambda(zP_+, \mathbf{k})\gamma_5 v_{\bar{\lambda}}((1-z)P_+, -\mathbf{k})\,\psi(z,\mathbf{k})$$

$$\psi(z,\mathbf{k}) = \frac{\pi}{\sqrt{2M_{c\bar{c}}}} \frac{u(p)}{p}\,.$$

Terentev prescription valid for weakly bound system
$\mathbf{p} = \mathbf{k}, \quad p_z = (z - \frac{1}{2})M_{c\bar{c}}, \; M^2_{c\bar{c}} = \frac{\mathbf{k}^2 + m_c^2}{z(1-z)}$.
Helicity dependence from Melosh-Trf. of RF-WF

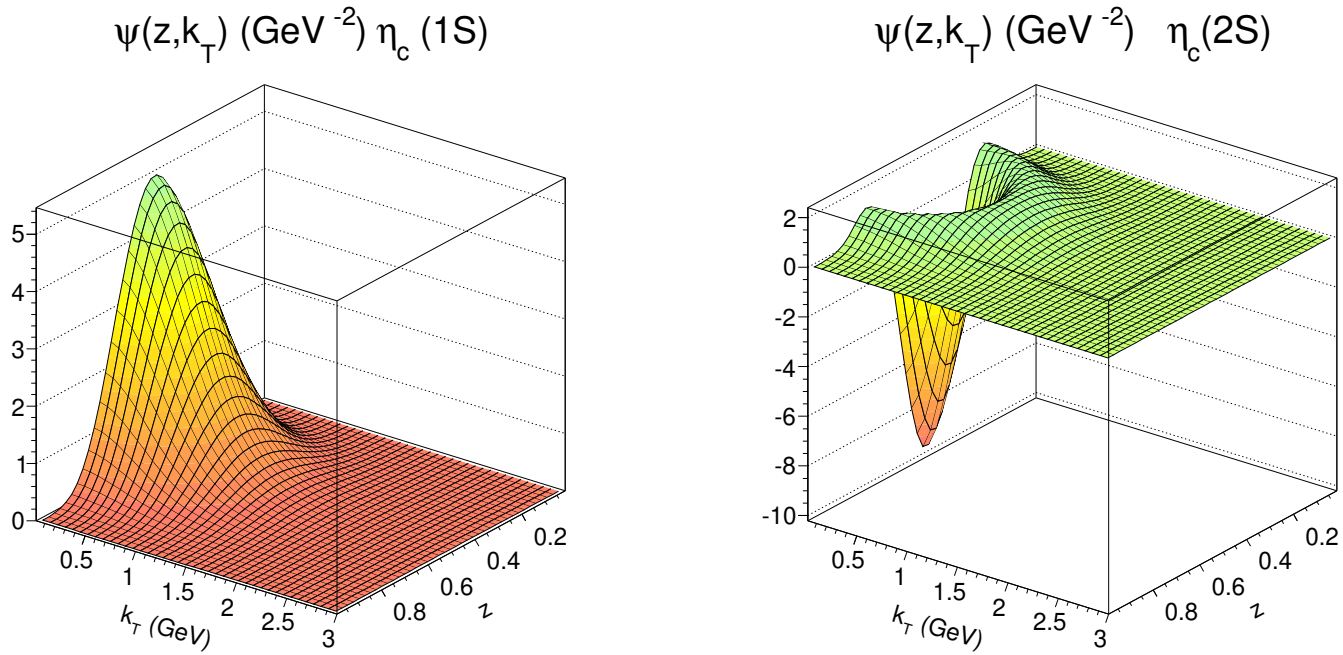

Radial light-front wave function for Buchmüller-Tye potential.

$F(0,0)$ transition for both on-shell photons

$$F(0,0) = e_c^2 \sqrt{N_c}\, 4m_c \cdot \int \frac{dz d^2\mathbf{k}}{z(1-z)16\pi^3} \frac{\psi(z,\mathbf{k})}{\mathbf{k}^2 + m_c^2} ,$$

$F(0,0)$ is related to the two-photon decay width by the formula:

$$\Gamma(\eta_c \to \gamma\gamma) = \frac{\pi}{4} \alpha_{\rm em}^2 M_{\eta_c}^3 \left|F(0,0)\right|^2 .$$

$F(0,0)$ can be rewrite in the terms of radial momentum space wave function $u(p)$:

$$F(0,0) = e_c^2 \sqrt{2N_c}\, \frac{2m_c}{\pi} \int_0^\infty \frac{dp\, p\, u(p)}{\sqrt{M_{c\bar{c}}^3 (p^2 + m_c^2)}} \frac{1}{2\beta} \log\left(\frac{1+\beta}{1-\beta}\right) ,$$

In the non-relativistic (NR) limit, where $p^2/m_c^2 \ll 1, \beta \ll 1$, and $2m_c = M_{c\bar{c}} = M_{\eta_c}$, we obtain

$$F(0,0) = e_c^2 \sqrt{N_c}\sqrt{2} \frac{4}{\pi\sqrt{M_{\eta_c}^5}} \int_0^\infty dp\, p\, u(p) = e_c^2 \sqrt{N_c} \frac{4\, R(0)}{\sqrt{\pi M_{\eta_c}^5}} ,$$

where $\beta = \frac{p}{\sqrt{p^2+m_c^2}}$, the velocity v/c of the quark in the $c\bar{c}$ cms-frame and R(0) radial wave function at the origin.

$F(0,0)$ for both on-shell photons: $\eta_c(1S)$

Transition form factor $|F(0,0)|$ for η_c**(1S)** at $Q_1^2 = Q_2^2 = 0$.

potential type	m_c [GeV]	$\lvert F(0,0)\rvert$ [GeV^{-1}]	$\Gamma_{\gamma\gamma}$ [keV]	f_{η_c} [GeV]
harmonic oscillator	1.4	0.051	2.89	0.2757
logarithmic	1.5	0.052	2.95	0.3373
power-like	1.334	0.059	3.87	0.3074
Cornell	1.84	0.039	1.69	0.3726
Buchmüller-Tye	1.48	0.052	2.95	0.3276
experiment	-	0.067 ± 0.003 [1]	5.1 ± 0.4 [1]	0.335 ± 0.075 [2]

[1] M. Tanabashi *et al.* [Particle Data Group], Phys. Rev. D **98**, no.3, 030001 (2018).

[2] K. W. Edwards *et al.* [CLEO Collaboration], Phys. Rev. Lett. **86**, 30 (2001) [hep-ex/0007012].

R(0) and $\gamma\gamma$-width for η_c**(1S)** derived in **the non-relativistic limit**.

potential type	R(0)[$\mathrm{GeV}^{3/2}$]	$\Gamma_{\gamma\gamma}$ [keV] $\mathrm{M} = \mathrm{M}_{\eta_c}$	$\Gamma_{\gamma\gamma}$ [keV] $\mathrm{M} = 2\mathrm{m_c}$
harmonic oscillator	0.6044	5.1848	5.8815
logarithmic	0.8919	11.290	11.157
power-like	0.7620	8.2412	10.297
Cornell	1.2065	20.660	13.568
Buchmüller-Tye	0.8899	11.240	11.409

- η_c decay constant:

$$f_{\eta_c} = \frac{-i}{p_+}\langle 0|\bar{c}(0)\gamma_+\gamma_5 c(0)|\eta_c(p_+)\rangle = \frac{\sqrt{N_c}\,4m_c}{16\pi^3}\int_0^1 \frac{dz}{z(1-z)}\int d^2\mathbf{k}\,\psi(z,\mathbf{k})$$

$F(0,0)$ for both on-shell photons: $\eta_c(2S)$

Transition form factor $|F(0,0)|$ for $\eta_c(2S)$ at $Q_1^2 = Q_2^2 = 0$.

potential type	m_c [GeV]	$\lvert F(0,0)\rvert$ [GeV^{-1}]	$\Gamma_{\gamma\gamma}$ [keV]	f_{η_c} [GeV]
harmonic oscillator	1.4	0.03492	2.454	0.2530
logarithmic	1.5	0.02403	1.162	0.1970
power-like	1.334	0.02775	1.549	0.1851
Cornell	1.84	0.02159	0.938	0.2490
Buchmüller-Tye	1.48	0.02687	1.453	0.2149
experiment [1]	-	0.03266 ± 0.01209	2.147 ± 1.589	

[1] M. Tanabashi *et al.* [Particle Data Group], Phys. Rev. D **98**, no.3, 030001 (2018).

R(0) and $\gamma\gamma$-width for $\eta_c(2S)$ derived in the **non-relativistic limit.**

potential type	R(0) [GeV$^{3/2}$]	$\Gamma_{\gamma\gamma}$ [keV] $\mathrm{M} = \mathrm{M}_{\eta_c}$	$\Gamma_{\gamma\gamma}$ [keV] $\mathrm{M} = 2\mathrm{m_c}$
harmonic oscillator	0.7402	5.2284	8.8214
logarithmic	0.6372	3.8745	5.6946
power-like	0.5699	3.0993	5.7594
Cornell	0.9633	8.8550	8.6493
Buchmüller-Tye	0.7185	4.9263	7.4374

Normalized transition form factor $\tilde{F}(Q^2, 0)$

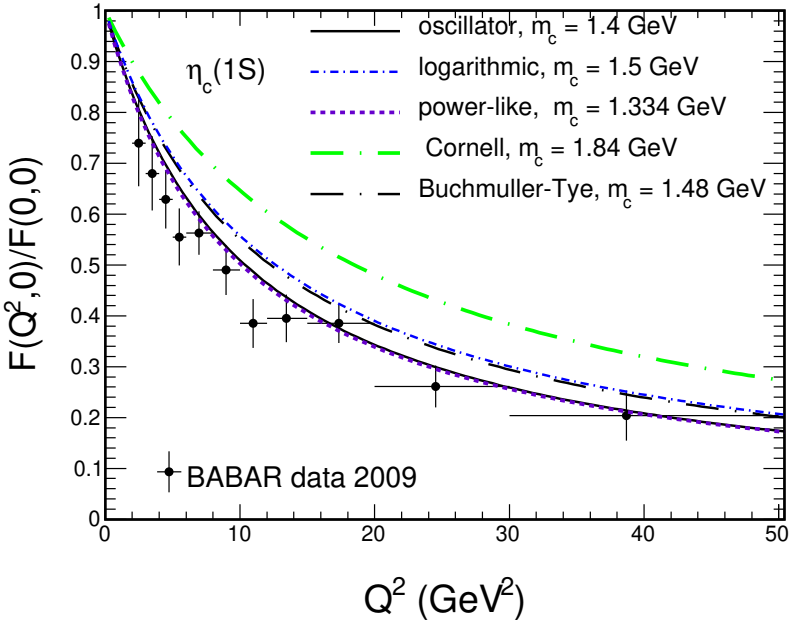

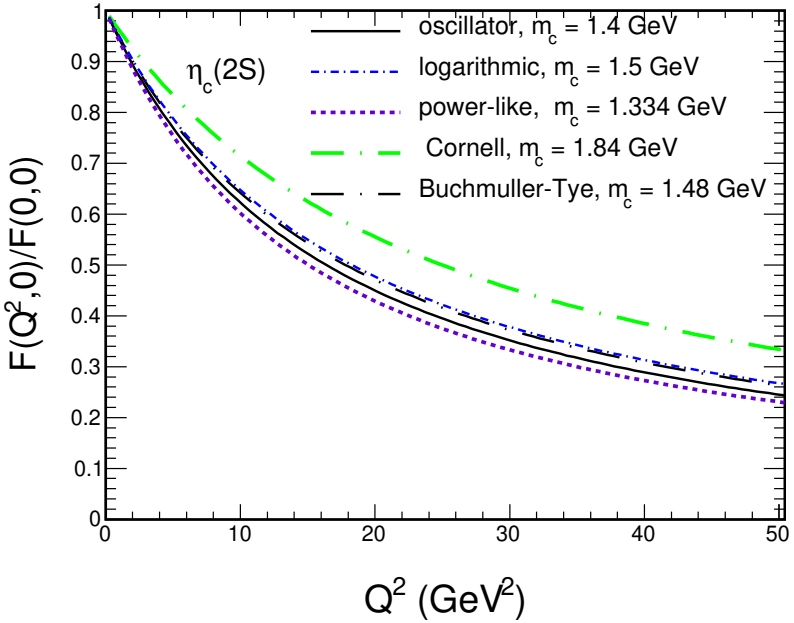

Normalized transition form factor $\tilde{F}(Q^2, 0)$ as a function of photon virtuality Q^2. The BaBar data are shown for comparison.

J. P. Lees *et al.* [BaBar Collaboration], Phys. Rev. D **81**, 052010 (2010) [arXiv:1002.3000 [hep-ex]].

Asymptotic behaviour of $Q^2F(Q^2,0)$

The rate of approaching of $Q^2F(Q^2,0)$ to its asymptotic value predicted by Brodsky and Lepage

G. P. Lepage and S. J. Brodsky, Phys. Rev. D **22**, 2157 (1980).

$Q^2F(Q^2,0) \to \frac{8}{3} f_{\eta_c}$, for $Q^2 \to \infty$

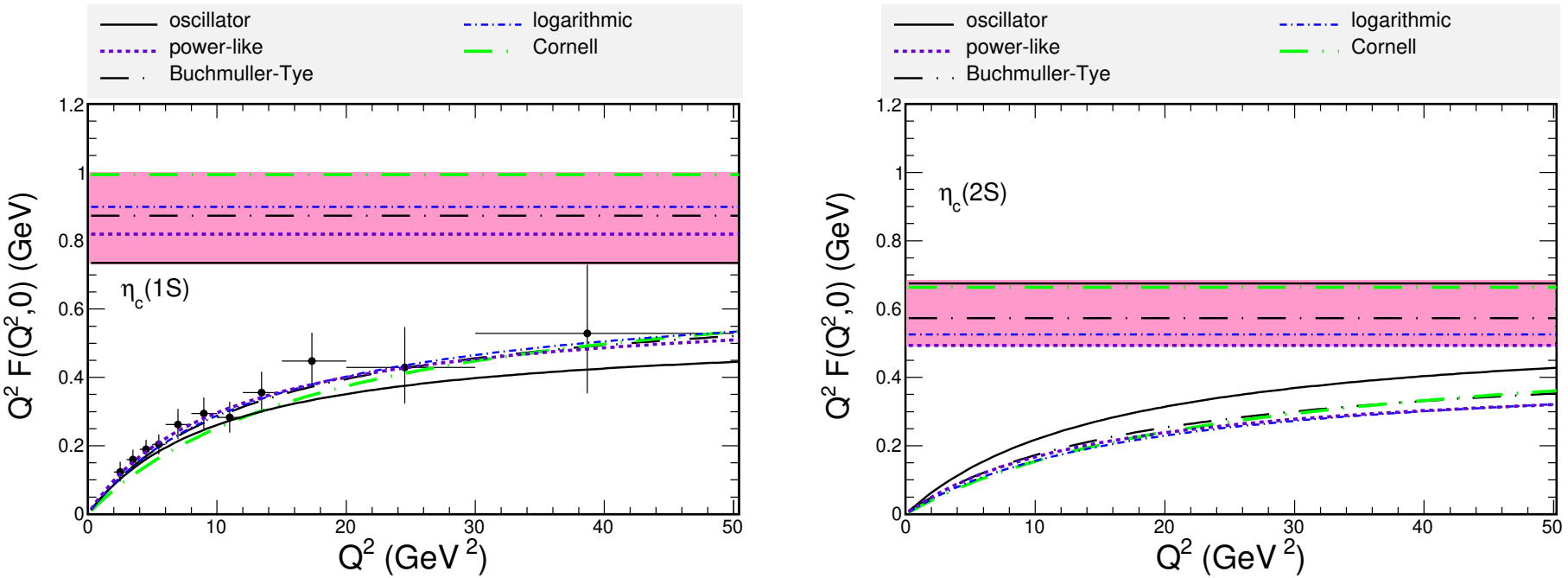

$Q^2F(Q^2,0)$ as a function of photon virtuality Q^2.Therefore the horizontal lines $\frac{8}{3} f_{\eta_c}$ are shown for reference.

- very far from the asymptotic limit.
- we also investigated RG evolution of the DA, which is however very slow.

Distribution amplitudes of $\eta_c(1S, 2S)$

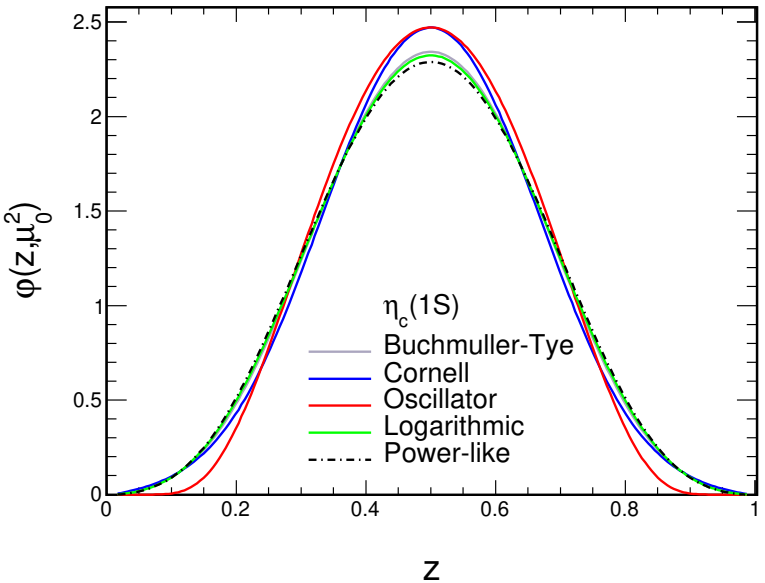

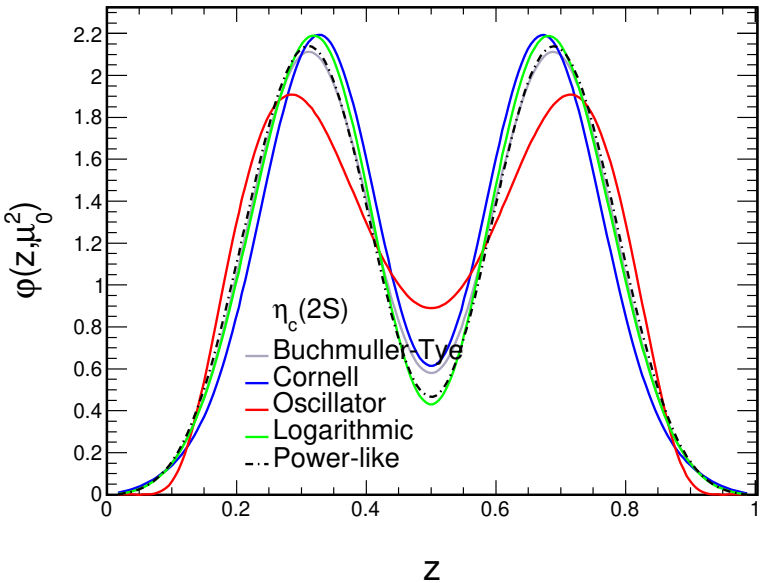

- distribution amplitudes for different wave functions for η_c (1S) (left panel) and for η_c (2S) (right panel).

$$f_{\eta_c}\varphi(z,\mu_0^2) \quad = \quad \frac{1}{z(1-z)}\frac{\sqrt{N_c}\,4m_c}{16\pi^3}\int d^2\mathbf{k}\,\theta(\mu_0^2-\mathbf{k}^2)\,\psi(z,\mathbf{k})$$

Transition form factor $F(Q_1^2, Q_2^2)\,\gamma^*\gamma^* \to \eta_c(1S, 2S)$

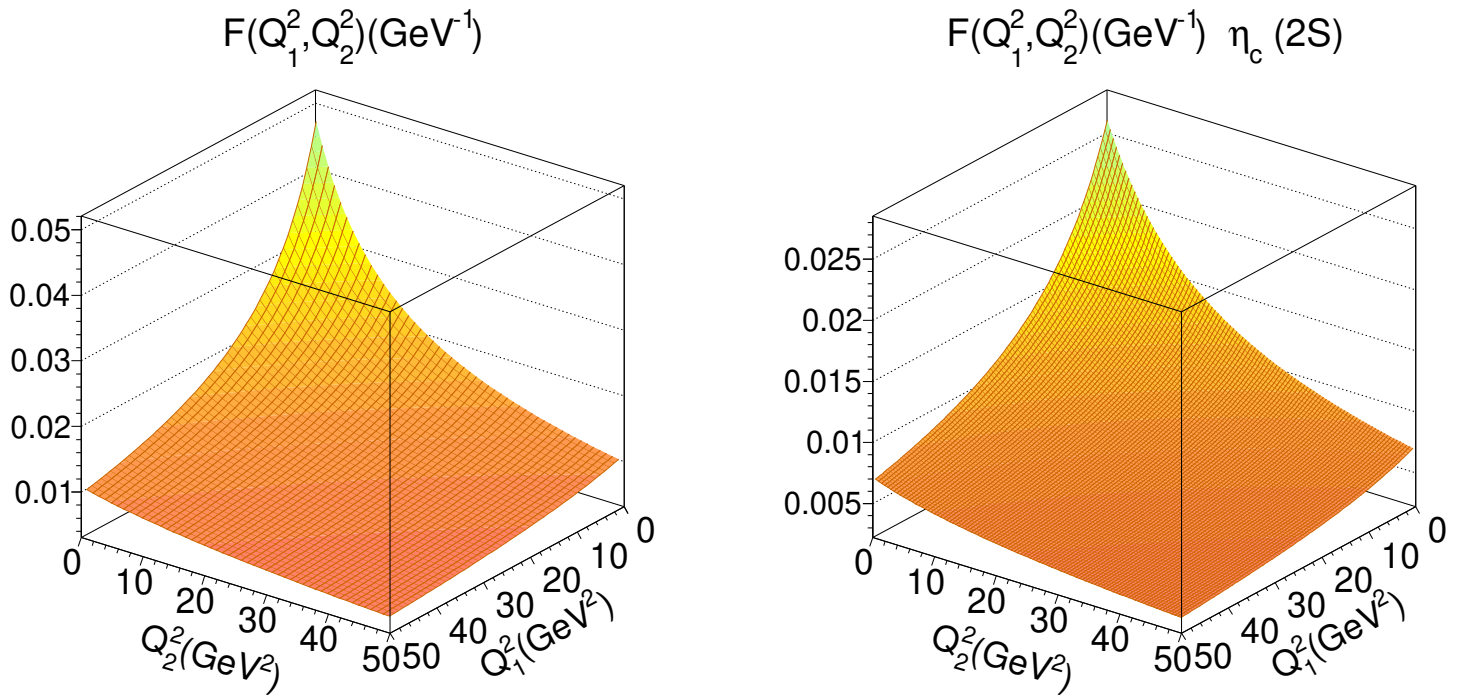

Transition form factor for $\eta_c(1S)$ and $\eta_c(2S)$ for Buchmüller -Tye potential. Bose symmetry $Q_1^2 \leftrightarrow Q_2^2$.

Transition form factor $F(\omega, \overline{Q^2})$

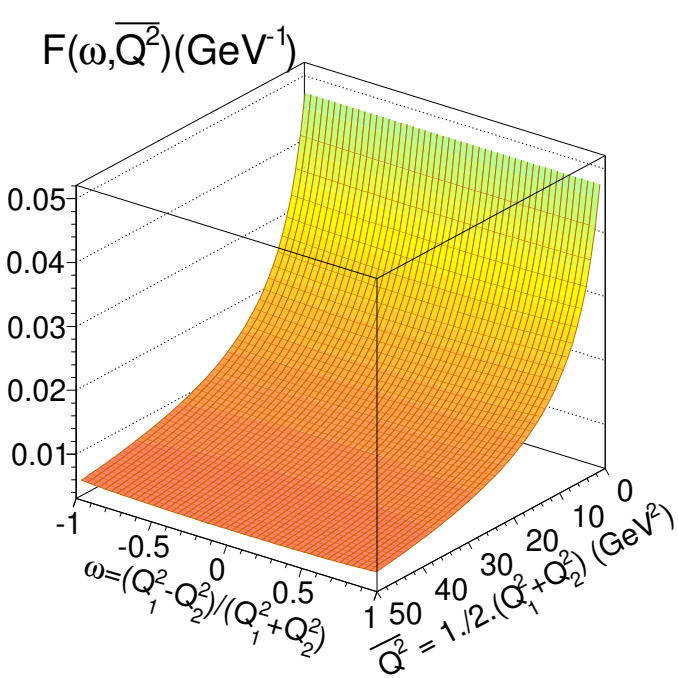

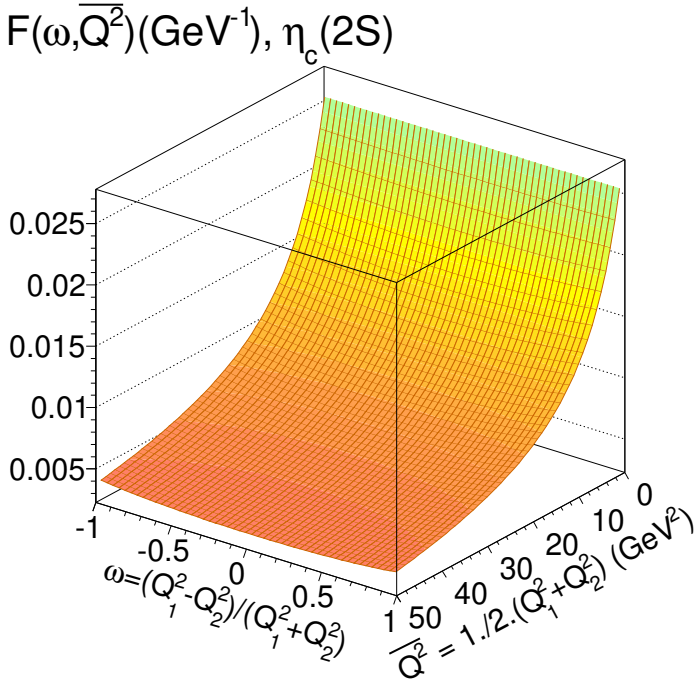

The $\gamma^*\gamma^* \to \eta_c$ (1S) and $\gamma^*\gamma^* \to \eta_c$ (2S) form factor as a function of (Q_1^2, Q_2^2) and $(\omega, \bar{Q}^2)$ for the Buchmüller-Tye potential for illustration.

$$\omega = \frac{Q_1^2 - Q_2^2}{Q_1^2 + Q_2^2} \quad \text{and} \quad \bar{Q}^2 = \frac{Q_1^2 + Q_2^2}{2} \, .$$

Hadroproduction of $\eta_c(1S, 2S)$ via gluon-gluon fusion

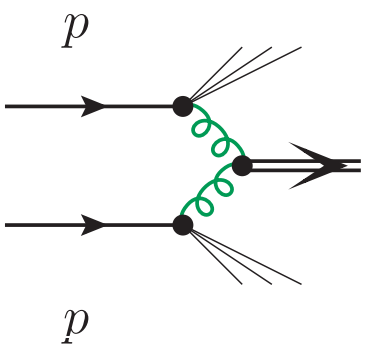

$$\frac{d\sigma}{dyd^2\boldsymbol{p}} = \int \frac{d^2\boldsymbol{q}_1}{\pi \boldsymbol{q}_1^2} \mathcal{F}(x_1, \boldsymbol{q}_1^2) \int \frac{d^2\boldsymbol{q}_2}{\pi \boldsymbol{q}_2^2} \mathcal{F}(x_2, \boldsymbol{q}_2^2) \times \delta^{(2)}(\boldsymbol{q}_1 + \boldsymbol{q}_2 - \boldsymbol{p}) \frac{\pi}{(x_1 x_2 s)^2} \overline{|\mathcal{M}|^2},$$

where the momentum fractions of gluons are fixed as $x_{1,2} = m_T \exp(\pm y)/\sqrt{s}$. The off-shell matrix element is written in terms of the Feynman amplitude as (we restore the color-indices):

Catani, Ciafaloni & Hautmann; Gribov, Levin & Ryskin, Collins & Ellis

$$\mathcal{M}^{ab} = \frac{q_{1\perp}^\mu q_{2\perp}^\nu}{|\boldsymbol{q}_1||\boldsymbol{q}_2|} \mathcal{M}_{\mu\nu}^{ab} = \frac{q_{1+} q_{2-}}{|\boldsymbol{q}_1||\boldsymbol{q}_2|} n_\mu^+ n_\nu^- \mathcal{M}_{\mu\nu}^{ab} = \frac{x_1 x_2 s}{2|\boldsymbol{q}_1||\boldsymbol{q}_2|} n_\mu^+ n_\nu^- \mathcal{M}_{\mu\nu}^{ab}.$$

In covariant form, the matrix element reads:

$$\mathcal{M}_{\mu\nu}^{ab} = (-i) 4\pi\alpha_s \varepsilon_{\mu\nu\alpha\beta} q_1^\alpha q_2^\beta \frac{Tr[t^a t^b]}{\sqrt{N_c}} I(\boldsymbol{q}_1^2, \boldsymbol{q}_2^2).$$

To the lowest order, it is proportional to the matrix element for the $\gamma^*\gamma^*\eta_c$ vertex. In particular, the form factor $I(\boldsymbol{q}_1^2, \boldsymbol{q}_2^2)$ is related to the $\gamma^*\gamma^*\eta_c$ transition form factor $F(Q_1^2, Q_2^2)$, $Q_i^2 = \boldsymbol{q}_i^2$ as

$$F(Q_1^2, Q_2^2) = e_c^2 \sqrt{N_c}\, I(\boldsymbol{q}_1^2, \boldsymbol{q}_2^2),$$

$$n_\mu^+ n_\mu^- \mathcal{M}_{\mu\nu}^{ab} = 4\pi\alpha_s(-i)[\boldsymbol{q}_1,\boldsymbol{q}_2]\frac{Tr[t^a t^b]}{\sqrt{N_c}}\, I(\boldsymbol{q}_1^2,\boldsymbol{q}_2^2) = 4\pi\alpha_s(-i)\frac{1}{2}\delta^{ab}\frac{1}{\sqrt{N_c}}[\boldsymbol{q}_1,\boldsymbol{q}_2]\, I(\boldsymbol{q}_1^2,\boldsymbol{q}_2^2)\,,$$

and averaging over colors, we obtain our final result:

$$\frac{d\sigma}{dyd^2\boldsymbol{p}} = \int \frac{d^2\boldsymbol{q}_1}{\pi\boldsymbol{q}_1^4}\mathcal{F}(x_1,\boldsymbol{q}_1^2)\int \frac{d^2\boldsymbol{q}_2}{\pi\boldsymbol{q}_2^4}\mathcal{F}(x_2,\boldsymbol{q}_2^2)\,\delta^{(2)}(\boldsymbol{q}_1+\boldsymbol{q}_2-\boldsymbol{p})\,\frac{\pi^3\alpha_s^2}{N_c(N_c^2-1)}\,|[\boldsymbol{q}_1,\boldsymbol{q}_2]\, I(\boldsymbol{q}_1^2,\boldsymbol{q}_2^2)|^2.$$

Parametrizing the transverse momenta as $\boldsymbol{q}_i = (q_i^x, q_i^y) = |\boldsymbol{q}_i|(\cos\phi_i, \sin\phi_i)$, we can write the vector product $[\boldsymbol{q}_1,\boldsymbol{q}_2]$ as

$$[\boldsymbol{q}_1,\boldsymbol{q}_2] = q_1^x q_2^y - q_1^y q_2^x = |\boldsymbol{q}_1||\boldsymbol{q}_2|\sin(\phi_1-\phi_2)\,.$$

In our numerical calculations presented below, we set the factorization scale to $\mu_F^2 = m_T^2$, and the renormalization scale is taken in the form:

$$\alpha_s^2 \to \alpha_s(\max\{m_T^2,\boldsymbol{q}_1^2\})\alpha_s(\max\{m_T^2,\boldsymbol{q}_2^2\})\,.$$

Normalization

$$\Gamma(\eta_c \to \gamma\gamma) = \Gamma_{\rm LO}(\eta_c \to \gamma\gamma)\left(1 - \frac{20-\pi^2}{3}\frac{\alpha_s}{\pi}\right),$$
$$\Gamma(\eta_c \to gg) = \Gamma_{\rm LO}(\eta_c \to gg)\left(1 + 4.8\,\frac{\alpha_s}{\pi}\right).$$

Table: Total decay widths as well as $|F(0,0)|$ obtained from Γ_{tot} using the next-to-leading order approximation (see Eq. (1)).

	Experimental values Γ_{tot} (MeV)	Derived from NLO $\lvert F(0,0)\rvert_{gg}[GeV^{-1}]$
$\eta_c(1S)$	31.9±0.7	0.119±0.001
$\eta_c(2S)$	11.3±3.2±2.9	0.053±0.010

Table: Radiative decay widths as well as $|F(0,0)|$ obtained from $\Gamma_{\gamma\gamma}$ using leading order and next-to-leading order approximation.

	Experimental values $\Gamma_{\gamma\gamma}$(keV)	Derived from LO $\lvert F(0,0)\rvert[GeV^{-1}]$	Derived from NLO $\lvert F(0,0)\rvert_{\gamma\gamma}[GeV^{-1}]$
$\eta_c(1S)$	5.0 ±0.4	0.067±0.003	0.079±0.003
$\eta_c(2S)$	1.9 ±1.3 $\cdot 10^{-4}\cdot\Gamma_{\eta_c(2S)}$	0.033±0.012	0.038±0.014

M. Tanabashi *et al.* [Particle Data Group], Phys. Rev. D **98**, no. 3, 030001 (2018).

Results in LHCb kinematics

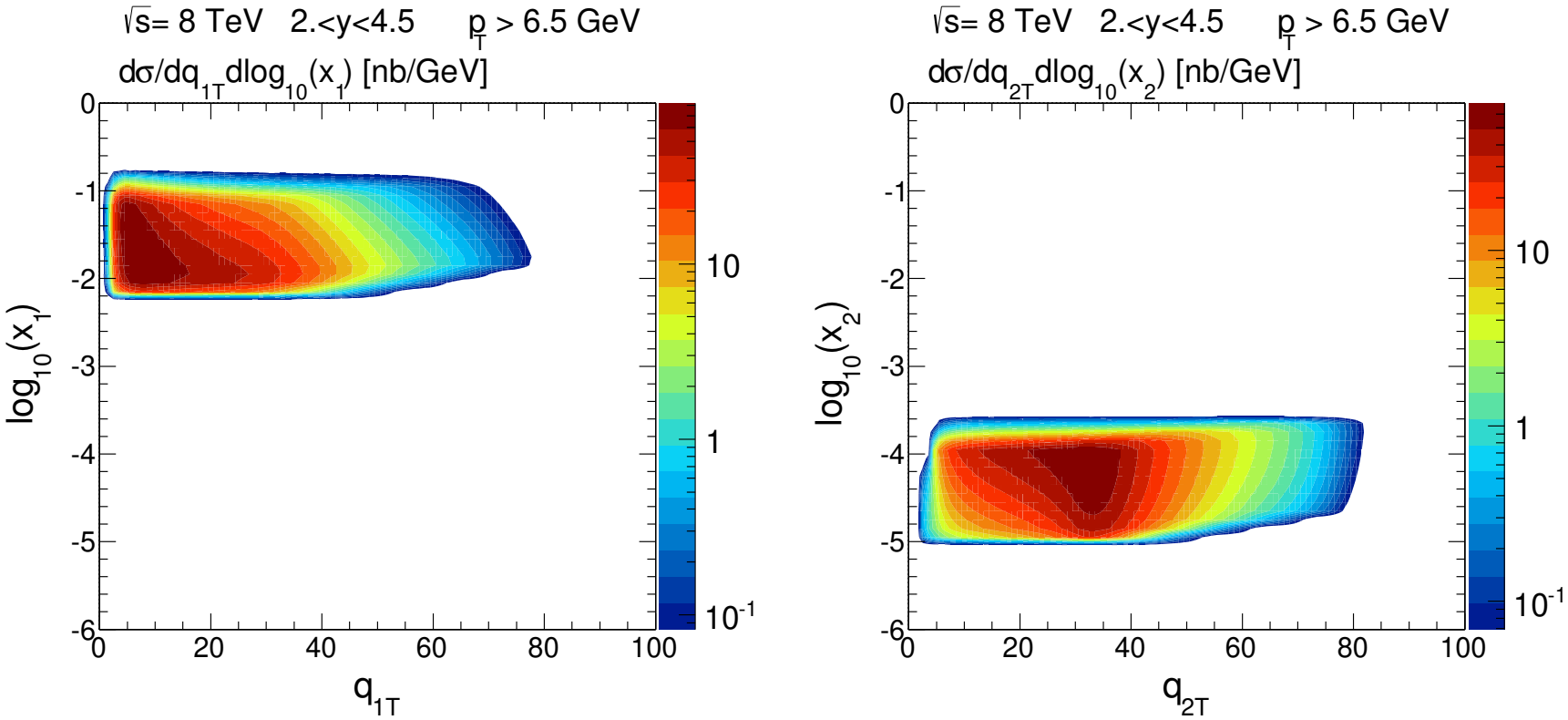

Figure: Two-dimensional distributions in (x_1, q_{1T}) (left panel) and in (x_2, q_{2T}) (right panel) for $\eta_c(1S)$ production for $\sqrt{s} = 8$ TeV. In this calculation the KMR UGD was used for illustration.

Results in LHCb kinematics

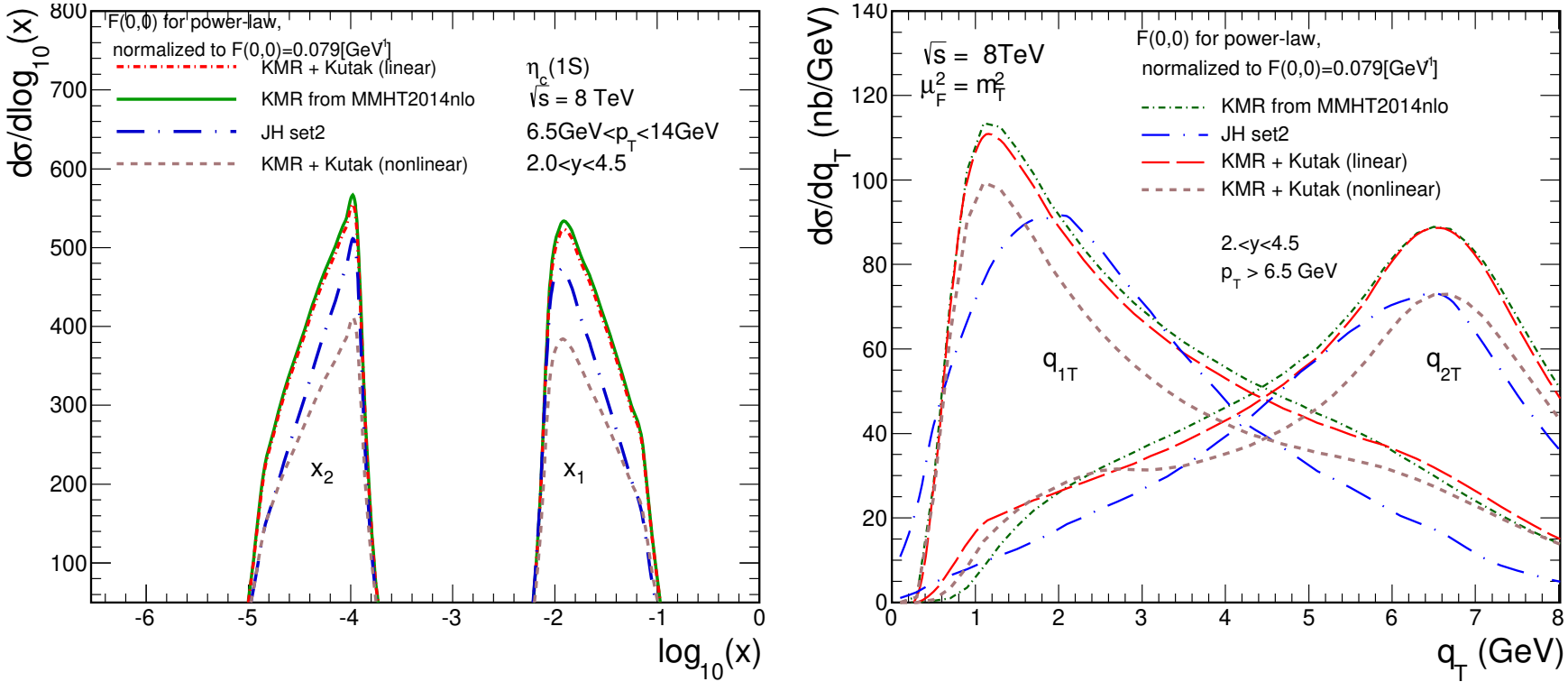

Figure: Distributions in $\log_{10}(x_1)$ or $\log_{10}(x_2)$ (left panel) and distributions in q_{1T} or q_{2T} (right panel) for the LHCb kinematics. Here the different UGDs were used in our calculations. Here we show an example, where $\sqrt{s} =$ 7 TeV.

Unintegrated gluon distributions

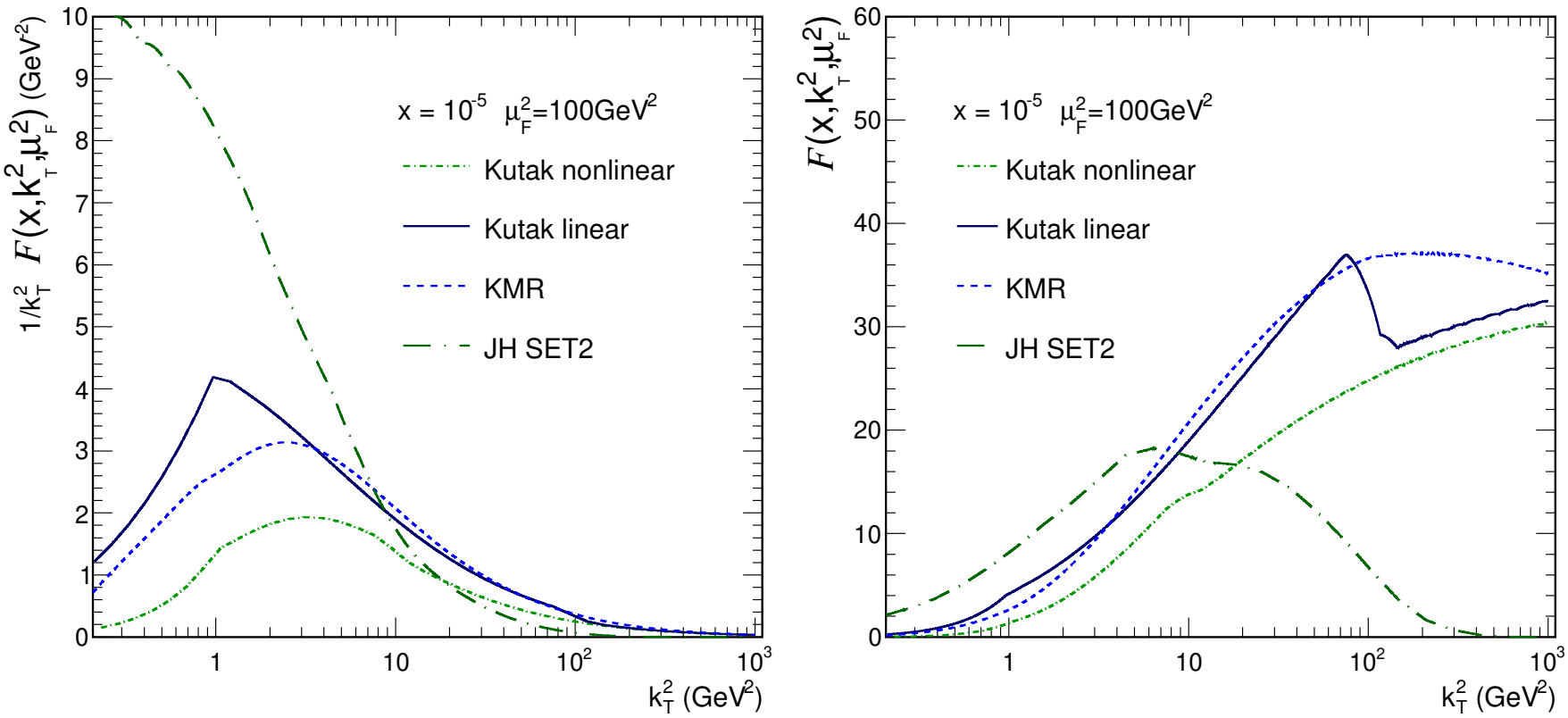

Figure: Unintegrated gluon densities for typical scale $\mu^2 = 100$ GeV^2 for $\eta_c(1S)$ production in proton-proton scattering at LHCb kinematics.

$$xg(x,\mu_F^2) = \int^{\mu_F^2} \frac{d\boldsymbol{k}^2}{\boldsymbol{k}^2} \mathcal{F}(x,\boldsymbol{k}^2,\mu_F^2)$$

p_T distributions in LHCb kinematics

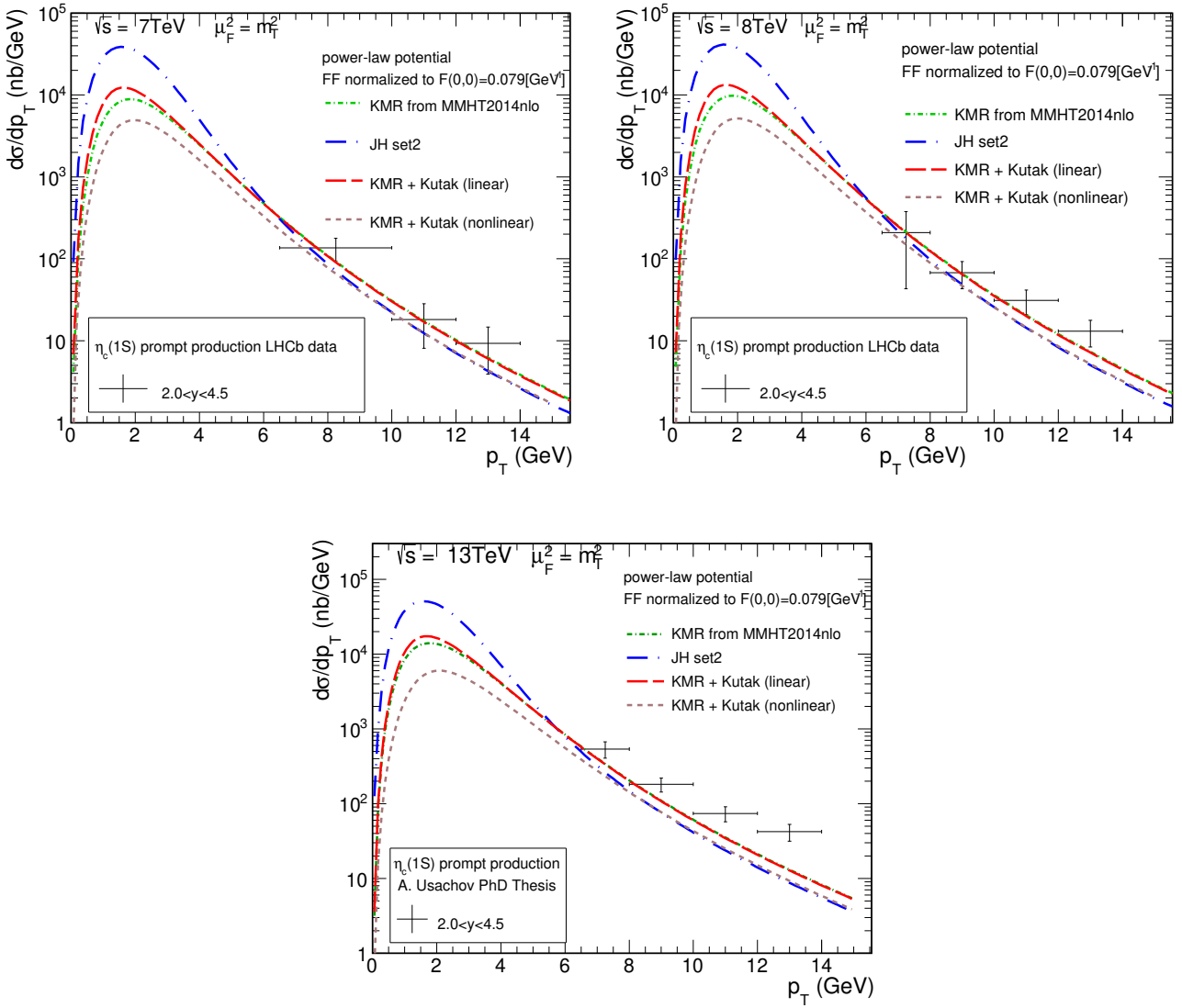

Figure: Differential cross section as a function of transverse momentum for prompt $\eta_c(1S)$ production compared with the LHCb data [1] for $\sqrt{s} = 7, 8\,\mathrm{TeV}$ and preliminary experimental data [2] for $\sqrt{s} = 13$ TeV. Different UGDs were used. Here we used the $g^* g^* \to \eta_c(1S)$ form factor calculated from the power-law potential.

Predictions for $\eta_c(2S)$

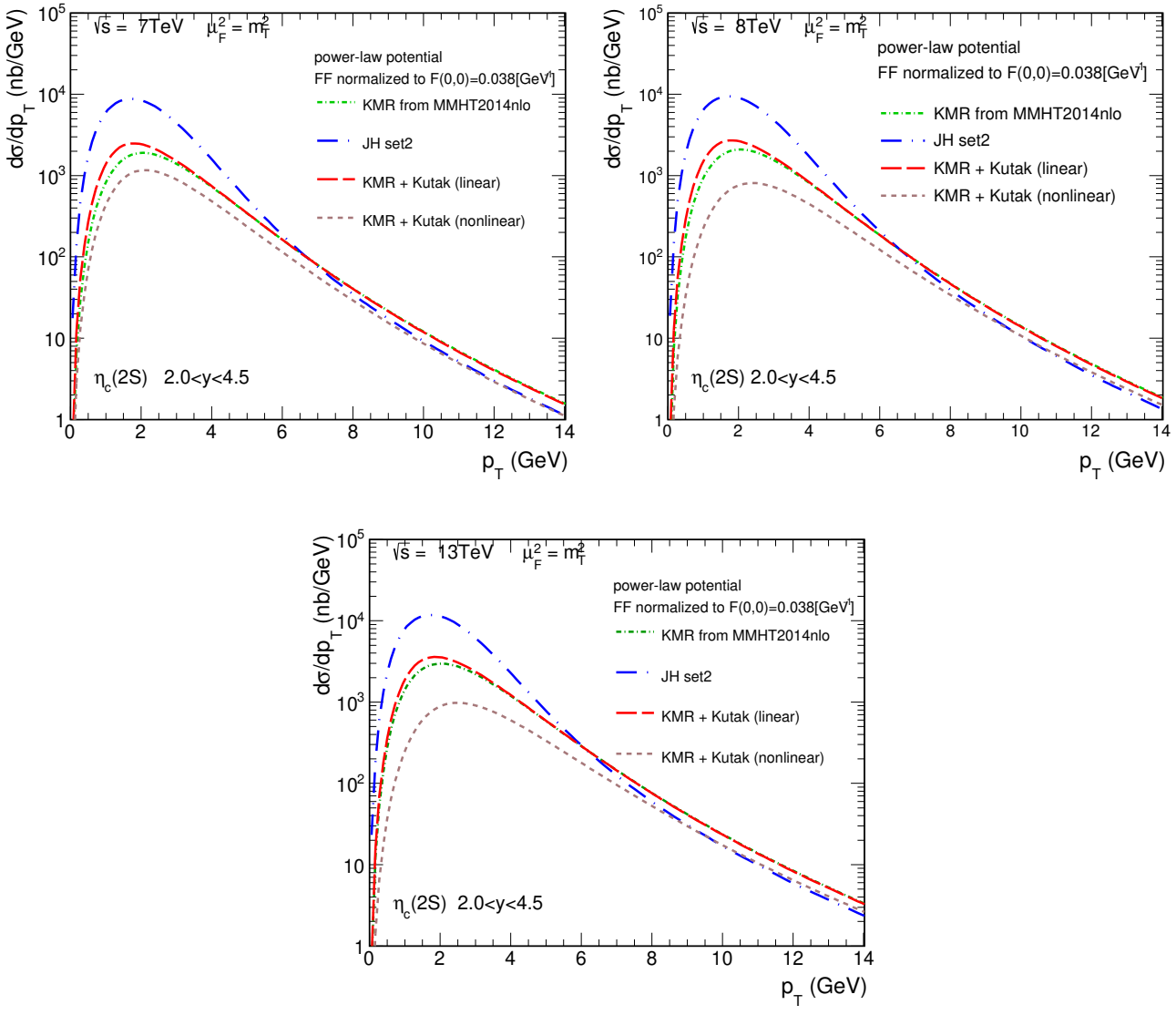

Figure: Differential cross section as a function of transverse momentum for prompt $\eta_c(2S)$ production for $\sqrt{s} = 7, 8, 13\,\mathrm{TeV}$.

Choice of the LFWF

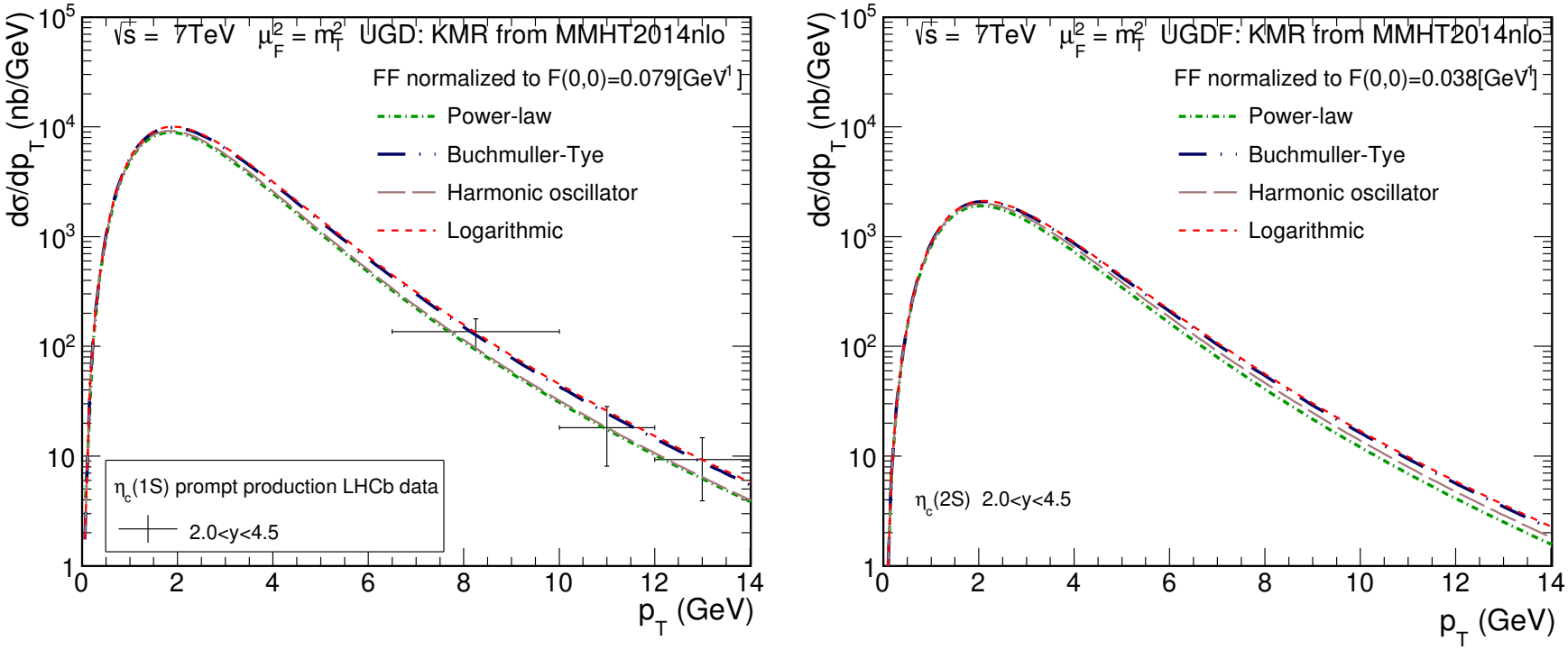

Figure: Transverse momentum distributions calculated with several different form factors obtained from different potential models of quarkonium wave function and one common normalization of $|F(0,0)|$.

Integrated cross section with LHCb cuts

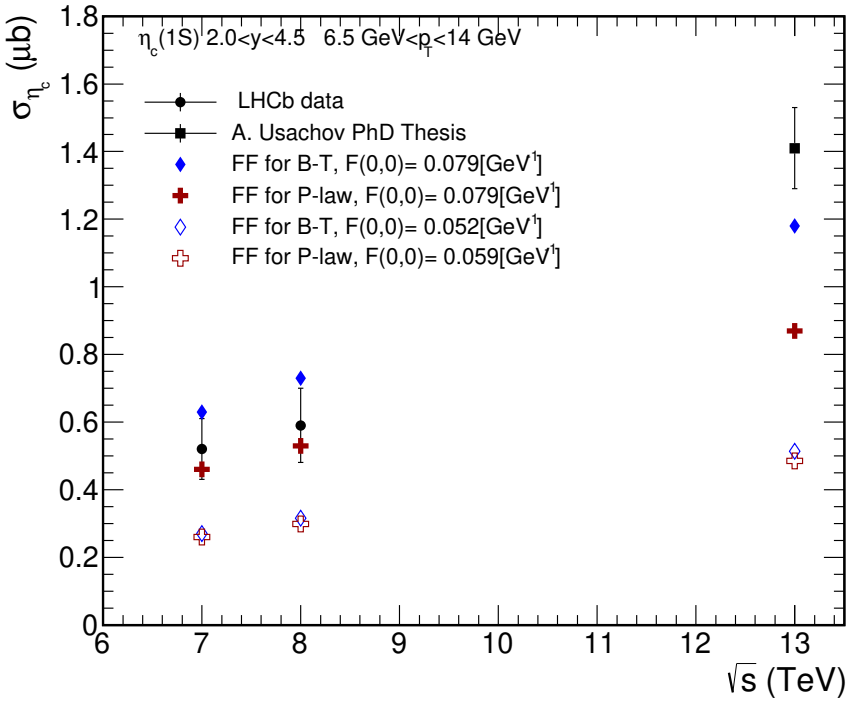

Figure: The integrated cross section computed within LHCb range of p_T and y with our transition form factors, compared to experimental values. Here red crosses represent values for Buchmüller-Tye potential (B-T) and deltoids for Power-law potential (P-law). Data are from [1],[2]

[1] R. Aaij *et al.* [LHCb Collaboration], Eur. Phys. J. C **75**, no. 7, 311 (2015).
[2] A. Usachov, PhD-thesis, "Study of charmonium production using decays to hadronic final states with the LHCb experiment," arXiv:1910.08796 [hep-ex].

Importance of the form factor

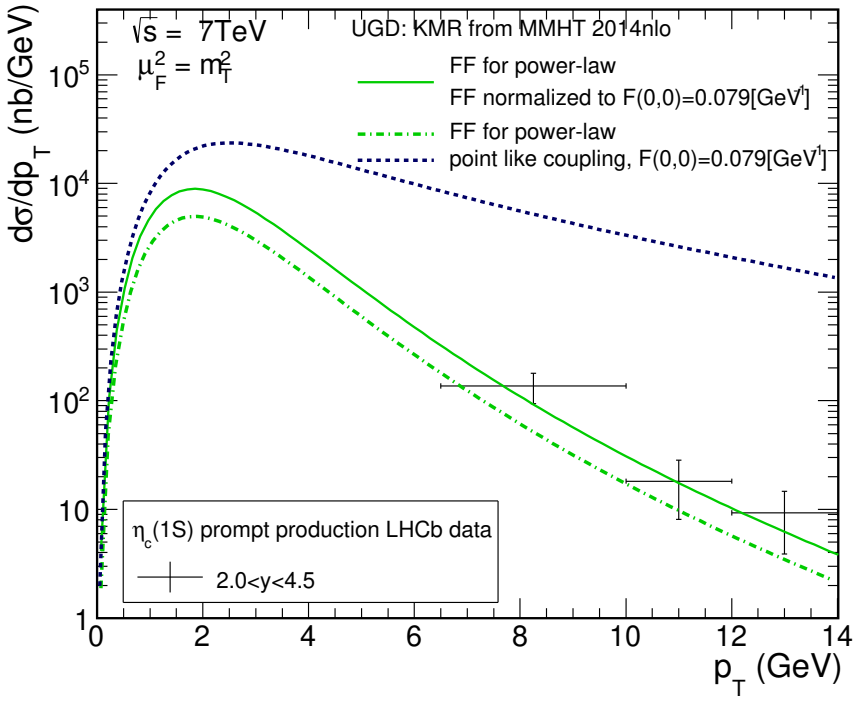

Figure: Comparison of results for two different transition form factor, computed with the KMR unintegrated gluon distribution. We also show result when the (q_{1T}^2, q_{2T}^2) dependence of the transition form factor is neglected.

- pointlike coupling of η_c to gluons $\propto \eta_c F^a_{\mu\nu} \tilde{F}^{a\mu\nu}$ badly overshoots data. Off-shell form factor is essential.

Results for ATLAS/CMS kinematics

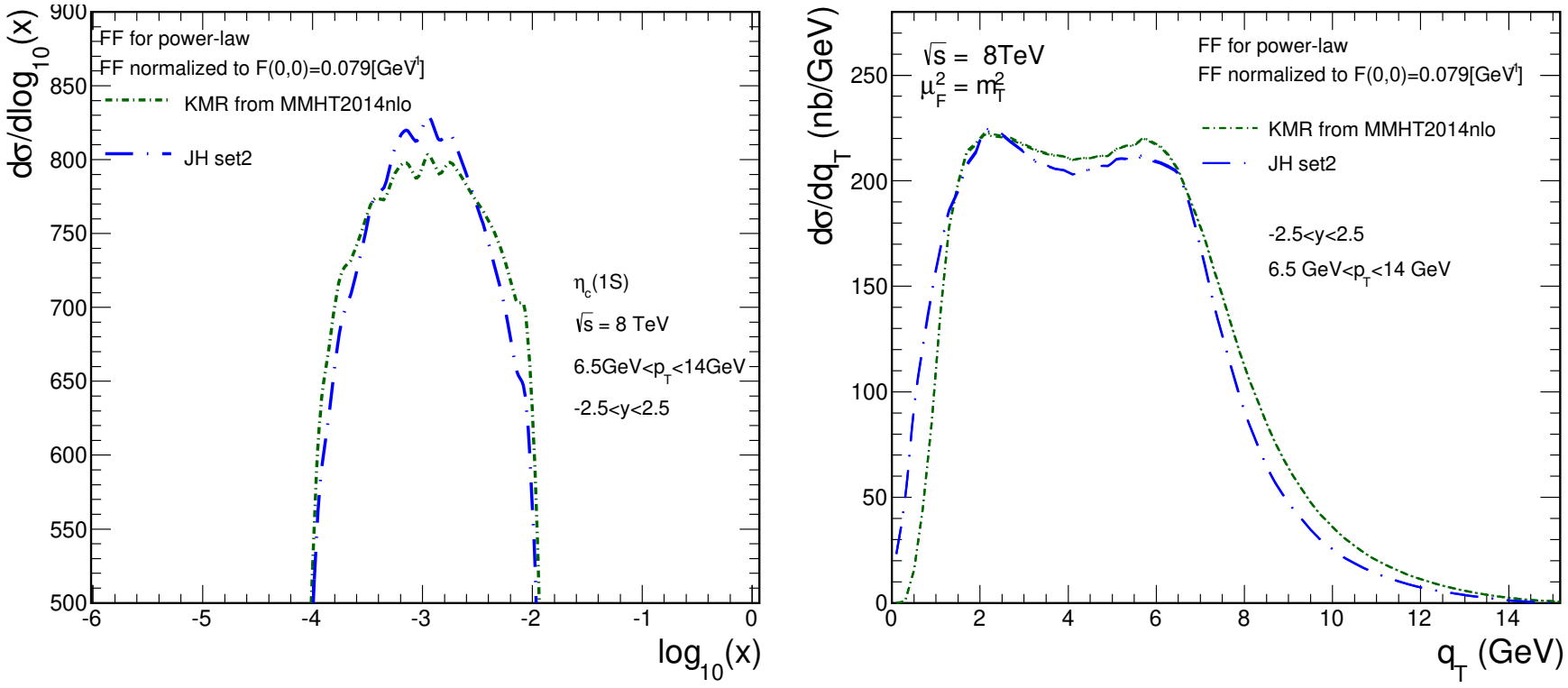

Figure: Distribution in $\log_{10}(x_1)$ or $\log_{10}(x_2)$ (left panel) and distribution in q_{1T} or q_{2T} (right panel) for ATLAS or CMS conditions.

Results for ATLAS/CMS kinematics

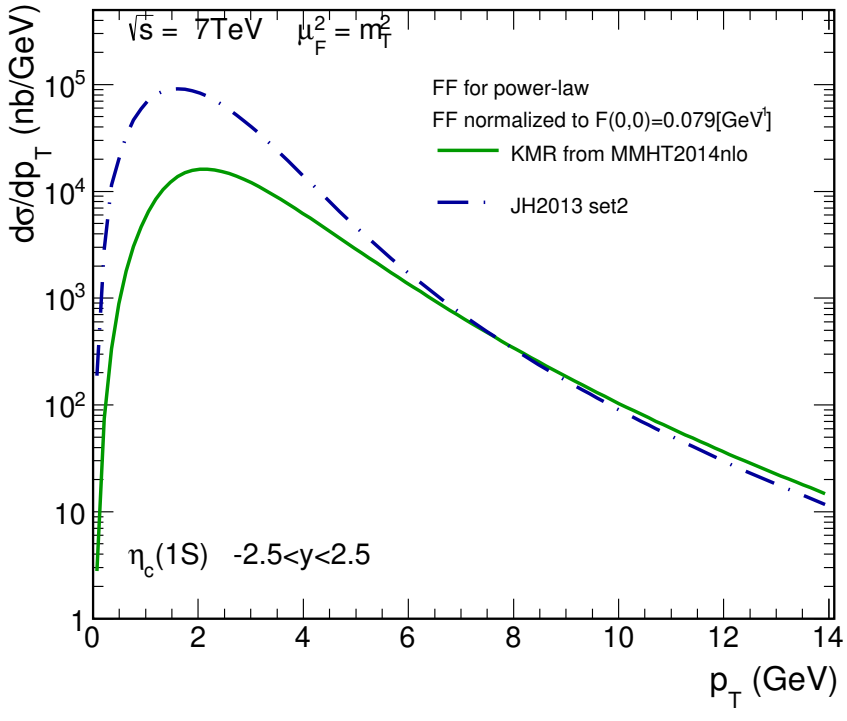

Figure: Transverse momentum distribution of prompt $\eta_c(1S)$ for $-2.5 < y < 2.5$ and $\sqrt{s}$ =7 TeV.

Hadroproduction of χ_{c0}, χ_{b0} via gluon-gluon fusion

$$\begin{aligned}\frac{d\sigma}{dyd^2\boldsymbol{p}} &= \int \frac{d^2\boldsymbol{q}_1}{\pi \boldsymbol{q}_1^2}\mathcal{F}(x_1,\boldsymbol{q}_1^2)\int \frac{d^2\boldsymbol{q}_2}{\pi \boldsymbol{q}_2^2}\mathcal{F}(x_2,\boldsymbol{q}_2^2)\,\delta^{(2)}(\boldsymbol{q}_1+\boldsymbol{q}_2-\boldsymbol{p})\frac{\pi^3\alpha_S^2}{N_c(N_c^2-1)} \\ &\times \left(G_1(\boldsymbol{q}_1^2,\boldsymbol{q}_2^2)+\cos(\phi_1-\phi_2)G_2(\boldsymbol{q}_1^2,\boldsymbol{q}_2^2)\right)^2,\end{aligned}$$

We parametrize the transverse momenta as $\boldsymbol{q}_i = (q_i^x, q_i^y) = |\boldsymbol{q}_i|(\cos\phi_i, \sin\phi_i)$.

$$\begin{aligned}G_1(\boldsymbol{q}_1^2,\boldsymbol{q}_2^2) &= |\boldsymbol{q}_1||\boldsymbol{q}_2|\,\frac{4m_Q}{\boldsymbol{q}_2^2}\int \frac{dzd^2\boldsymbol{k}}{z(1-z)16\pi^3}\psi(z,\boldsymbol{k})\,2z(1-z)(2z-1)\left[\frac{1}{\boldsymbol{l}_A^2+\varepsilon^2}-\frac{1}{\boldsymbol{l}_B^2+\varepsilon^2}\right] \\ G_2(\boldsymbol{q}_1^2,\boldsymbol{q}_2^2) &= 4m_Q\int \frac{dzd^2\boldsymbol{k}}{z(1-z)16\pi^3}\psi(z,\boldsymbol{k})\left[\frac{1-z}{\boldsymbol{l}_A^2+\varepsilon^2}+\frac{z}{\boldsymbol{l}_B^2+\varepsilon^2}\right] \\ &+ \frac{4m_Q}{\boldsymbol{q}_2^2}\int \frac{dzd^2\boldsymbol{k}}{z(1-z)16\pi^3}\psi(z,\boldsymbol{k})4z(1-z)\left[\frac{\boldsymbol{q}_2\cdot\boldsymbol{l}_A}{\boldsymbol{l}_A^2+\varepsilon^2}-\frac{\boldsymbol{q}_2\cdot\boldsymbol{l}_B}{\boldsymbol{l}_B^2+\varepsilon^2}\right].\end{aligned}$$

$$\varepsilon^2 = z(1-z)\boldsymbol{q}_1^2+m_Q^2\,,\qquad \boldsymbol{l}_A=\boldsymbol{k}-(1-z)\boldsymbol{q}_2\,,\qquad \boldsymbol{l}_B=\boldsymbol{k}+z\boldsymbol{q}_2\,.$$

- Form factors G_1, G_2 are linear combinations of the helicity form factors F_{TT}, F_{LL}.

$\gamma^*\gamma^*\chi_{c0}$ form factors

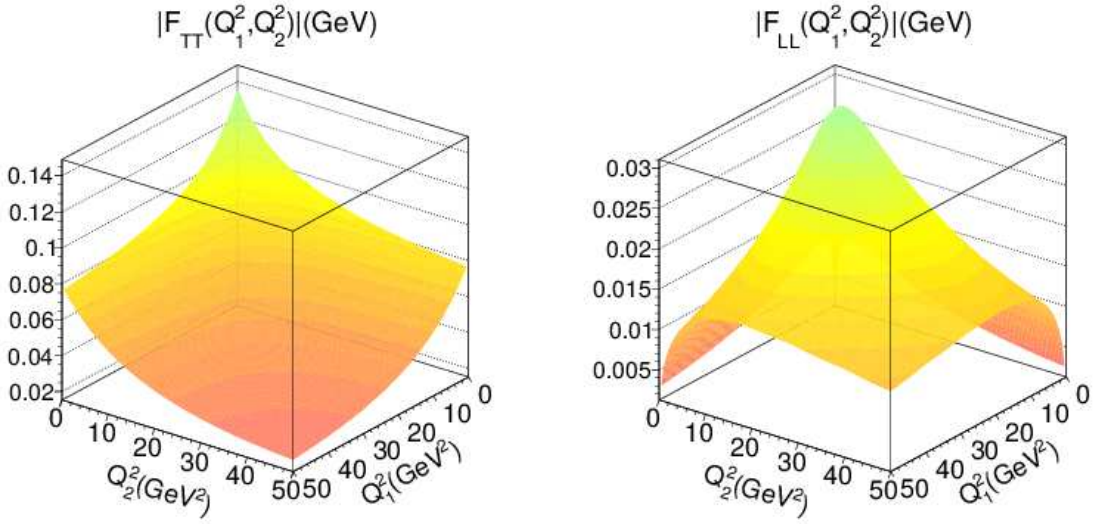

Figure: $|F_{TT}|$ (left) and F_{LL} (right) form factors for the Buchmüller-Tye potential for χ_{c0}.

$F_{TT}(0,0)$ with $m_c = 1.27\,\mathrm{GeV}$ and corresponding radiative widths.

Potential type	$\lvert F_{TT}(0,0)\rvert[GeV]$	$\Gamma(\chi_{c0}\to\gamma\gamma)_{LO}[keV]$	$\Gamma(\chi_{c0}\to\gamma\gamma)_{NLO}[keV]$
Harmonic oscillator	0.21	2.06	2.09
Logarithmic	0.18	1.54	1.56
Power-law	0.18	1.54	1.56
Cornell	0.17	1.41	1.43
Buchmüllller-Tye	0.18	1.54	1.56
extracted from experiment	0.21		2.20 ± 0.16

$\gamma^*\gamma^*\chi_{c0}$ form factors

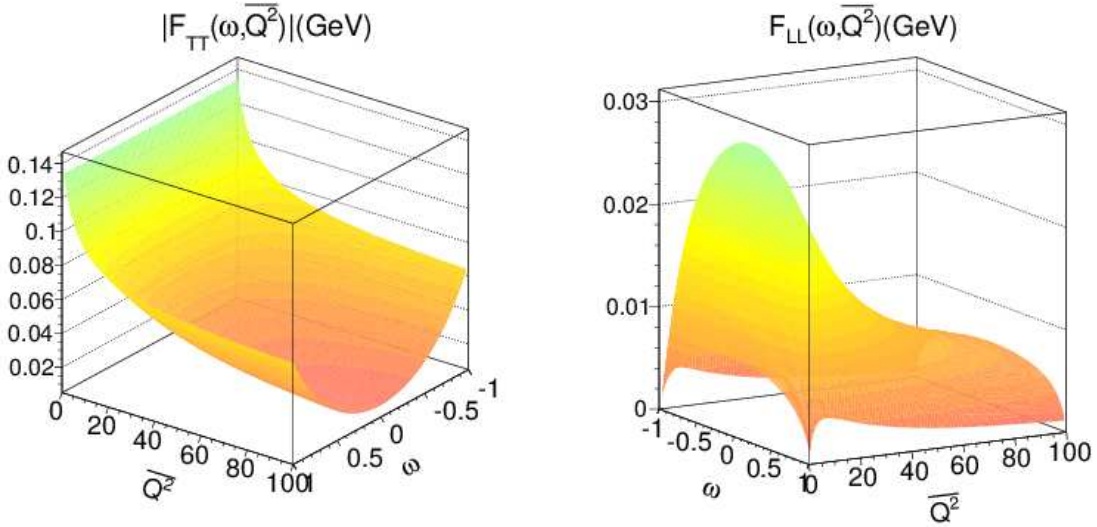

Figure: $|F_{TT}|$ (left) and F_{LL} (right) form factors for the Buchmüller-Tye potential as a function of ω and $\bar{Q}^2$ for χ_{c0}.

- rather strong functions of $\omega = (Q_1^2 - Q_2^2)/(Q_1^2 + Q_2^2)$.

Cross sections for hadroproduction of χ_{c0}, χ_{b0}

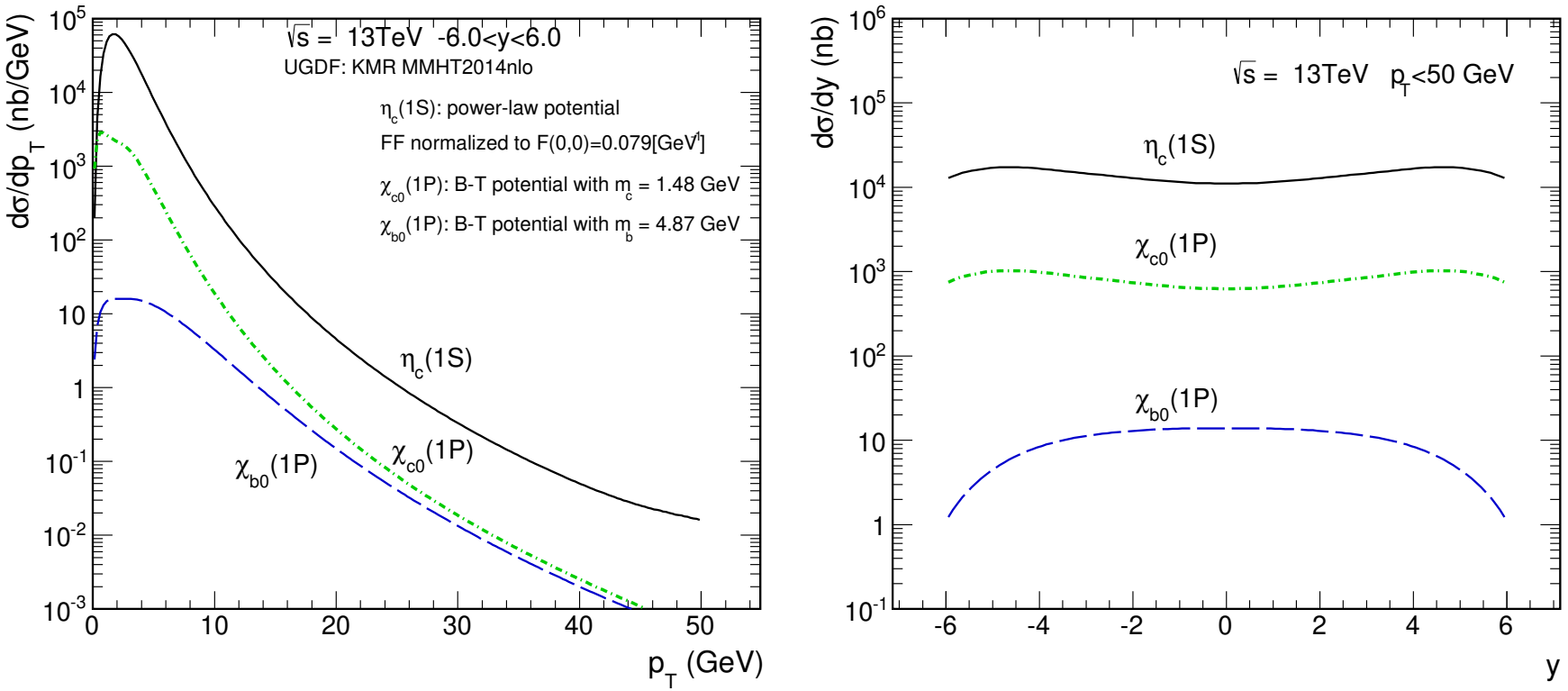

Figure: Differential cross section in terms of transverse momentum (lhs) and rapidity (rhs) of the meson (η_c, χ_{c0}, χ_{b0}).

Gluon polarizations: transverse vs. longitudinal

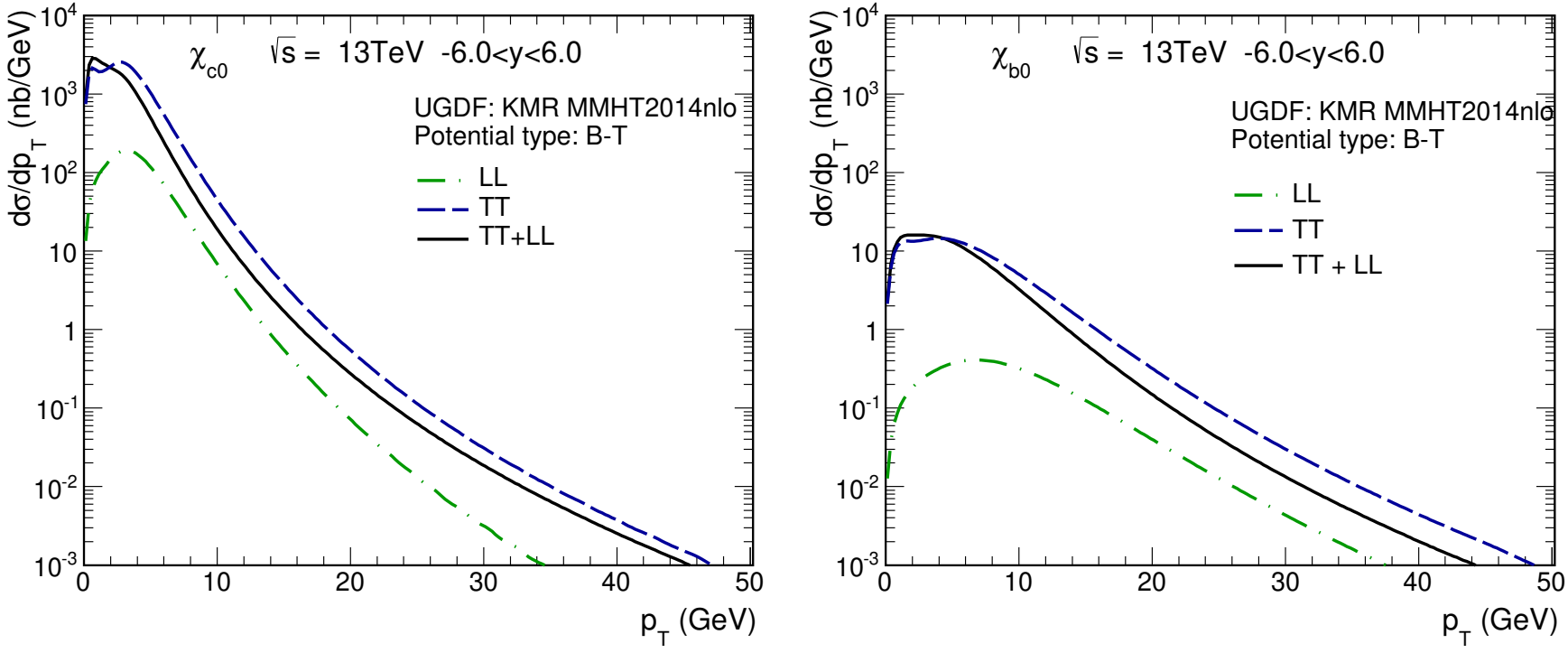

Figure: The comparison of meson transverse momentum distribution with only the *LL* amplitude and only *TT* amplitude as well as for the full, coherent sum of *TT* and *LL* amplitudes. Here the B-T potential was used.

- production of scalar particle probes a density matrix of transverse (linear - along the gluon transverse mom.) and longitudinal polarizations of gluons.

Conclusions

- The $\gamma^*\gamma^*$ transition form factors for different wave functions obtained as a solution of the Schrödinger equation for the $c\bar{c}$ system for different phenomenological $c\bar{c}$ potentials from the literature, was calculated.
- We have studied the transition form factors for $\gamma^*\gamma^* \to \eta_c$ (1S,2S) for two space-like virtual photons, which can be accessed experimentally in future measurements of the cross section for the $e^+e^- \to e^+e^-\eta_c$ process in the double - tag mode.
- For the $\eta_c(1S)$, the transition form factor for only one off-shell photon as a function of its virtuality,was studied and compared to the BaBar data.
- For the η_c there is practically no dependence on the asymmetry parameter ω, which could be verified experimentally at Belle 2.
- k_T-factorization approach with modern UGDs leads to good description of LHCb data for inclusive $pp \to \eta_c$ for $\sqrt{s} = 7, 8$ TeV, and somewhat worse for $\sqrt{s} = 13$ TeV (prelim. data). Some room for a color octet contribution is left.
- In the LHCb kinematics very small x are probed. Asymmetric kinematics where the small-x gluon transfers bulk of p_T.
- Despite sensitivity to small x, no sign of gluon saturation is observed. Integrated cross section grows even faster than the predictions without saturation.
- Predictions for $\eta_c(2S)$. A measurement could help to pin down possible color octet.
- Uncertainty due to $g^*g^*\eta_c, \chi_c$ form factors somewhat smaller than the one from UGD.
- For the case of χ_{c0}, χ_{b0} a gluon density matrix of transverse and longitudinal polarizations are probed.
- Predictions for χ_{c0}, χ_{b0} at LHC. Difficult to measure?